

Modification of Spacecraft Charging and the Near-Plasma Environment Caused by the Interaction of an Artificial Electron Beam With the Earth's Upper Atmosphere.

T. NEUBERT¹, P. M. BANKS¹, B. E. GILCHRIST¹, A. C. FRASER-SMITH¹,
P. R. WILLIAMSON¹, W. J. RAITT², N. B. MYERS², AND S. SASAKI³

Abstract. The Beam-Atmosphere Interaction (BAI) involves the ionization created in the earth's upper atmosphere by electron beams emitted from a low altitude spacecraft. This process is described by two coupled non-linear differential electron transport equations for the up-going (along a magnetic field line) and down-going differential energy flux. The equations are solved numerically, using the MSIS atmospheric model and the IRI ionospheric model, yielding estimates of the differential electron energy flux density at the spacecraft location. At altitudes below 200-250 km and for beam energies around 1 keV, it is shown that secondary electrons supply a significant contribution to the return current to the spacecraft and thereby reduce the spacecraft potential. Our numerical results are in good agreement with observations from the CHARGE-2 sounding rocket experiment. A more detailed study of the BAI as it relates the CHARGE-2 observations are found in [Neubert *et al.*, 1990].

1. INTRODUCTION

The return current to an electron beam-emitting spacecraft will, in general, have two components arising from completely different processes. The first component is the "classic" current that flows from the ambient plasma to a charged conductor, which we will refer to as the passive current [Langmuir and Blodgett, 1924; Beard and Johnson, 1961; Parker and Murphy, 1967]. The second component, the active current, relies on the electron beam or the charged spacecraft as a generator of return current electrons. Experiments performed from the space shuttle [Waterman *et al.*, 1988] and rockets [Winckler *et al.*, 1975; Myers *et al.*, 1989] have pointed out the importance of this component. The active current may be generated by a Beam-Plasma Interaction (BPI), a Beam-Plasma Discharge (BPD), a Beam-Atmosphere Interaction (BAI), or a Penning type discharge (PD). For a review see Linson [1982].

The CHARGE-2 tethered rocket experiment has provided the first direct measurements allowing to differentiate between the active and passive components of the return current, at least for the altitude range from 160 - 260 km [Myers *et al.*, 1989; Gilchrist *et al.*, 1990]. The observations indicated to us that the BAI was a likely candidate for the generation mechanism of the active current. Furthermore, quantitative estimates of the electron fluxes and electron energy spectra generated as a result of this process are possible and has been done for the case of energetic auroral electrons precipitating in the earth's upper atmosphere [Banks *et al.*, 1974].

This paper presents a summary of the results presented at the conference on spacecraft charging held in Monterey in October, 1989. A more detailed presentation is given in Neubert *et al.* [1990]. The following section describes briefly the CHARGE-2 experiment and the observations of the return currents to the spacecraft during electron beam emissions. Then follows a description of the method developed to study electron fluxes generated by artificial electron beams. Finally, we

¹ STAR LABORATORY, DEPARTMENT OF ELECTRICAL ENGINEERING STANFORD UNIVERSITY, STANFORD, CA 94305-4055

² CENTER FOR ATMOSPHERIC AND SPACE SCIENCES, UTAH STATE UNIVERSITY, LOGAN, UT 84322-4405

³ INSTITUTE FOR SPACE AND ASTRONAUTICAL SCIENCES, TOKYO 153, JAPAN

model the BAI return current for the CHARGE-2 experiment and find good agreement between observed and modeled currents.

2. THE CHARGE-2 EXPERIMENT

The CHARGE-2 payload consisted of two sections, a Mother and a Daughter section, which were electrically connected by an insulated tether. The experiment was designed to study phenomena related to electron beam emissions from spacecraft as well as the electrodynamic interaction of a tethered system with ambient ionospheric plasmas [Sasaki *et al.*, 1988]. During the flight, the two sections drifted apart in a direction roughly perpendicular to the spacecraft velocity and to the earth's magnetic field. Apogee was at 261 km altitude and the maximum separation distance of the two payloads was 426 m, reached at the end of the flight.

A schematic drawing of the CHARGE-2 payload is shown in Figure 1. The Mother carried an electron beam accelerator emitting beams with electron energies of 1 keV and currents up to 48 mA. Return currents were collected by both the Mother (I_M) and the Daughter (I_D) during beam injections. The electron beam current (I_{beam}) was measured by a Rogowski coil and the tether current (I_{tether}) was measured by a tether current monitor. Assuming that the beam escaped the Mother payload, we have $I_D = I_{tether}$ and $I_M = I_{beam} - I_{tether}$.

The tether impedance was relatively low (4 k Ω) in certain experimental sequences and the tether current was typically less than 6 mA. As a consequence, the potential difference between the two payloads was less than 24 V and small compared to the potentials of 200-600 V reached by the Mother payload. Thus the two payloads were at almost the same potential during these particular sequences. Since the Daughter was separated by up to several hundred meters from the Mother in the direction perpendicular to the earth's magnetic field and therefore was well outside of the disturbed region around the beam column, the Daughter return current represents a measurement of the passive return current. The return current to the Mother contains both a passive and an active component.

Figure 2 shows the fraction of the beam current collected by the Daughter as a function of altitude. The labels SQ2 through SQ6 mark the beam emission sequences performed during the flight numbered in time-sequential order. Also indicated is the ratio of the Daughter collecting area to the collecting area of both payloads, A_D/A_{total} . At high altitudes, around 250 km, the tether current approaches 0.3 times the beam current. This value is close to A_D/A_{total} , indicating that the two payloads collect return currents roughly in proportion to their areas, which is to be expected for passive current collection. Thus at high altitudes, where the ambient plasma density is large and the neutral density is low, the payloads mainly collect currents from the ambient plasma. The return currents and corresponding spacecraft potentials observed during the flight have been found in accordance with the model of Parker and Murphy [Myers *et al.*, 1989; Mandell *et al.*, 1990].

As the altitude decreases, the current collected by the Daughter decreases such that by an altitude of 180 km and below almost no current is collected by the Daughter. Assuming that the beam escapes the near environment of the Mother payload, we conclude that the active component of the return current, which flows directly to the Mother, increases with decreasing altitude. Since the ambient neutral atmospheric density also increases with decreasing altitude, such an altitude dependence is suggestive of a BAI process. In the following section we describe the method developed to quantify the fluxes generated by BAI.

3. THE BEAM-ATMOSPHERE INTERACTION MODEL

The code developed to study the interaction of an electron beam with the earth's upper atmosphere solves two coupled first order non-linear differential equations in the forward and the backward flux of electrons streaming in the direction of the ambient magnetic field. The equations coupling the forward differential energy flux, Φ^+ , and the backward flux, Φ^- , are given by

$$\frac{d\Phi^+(z, E)}{dz} = -\sigma_2(z, E)\Phi^+(z, E) + \sigma_1(z, E)\Phi^-(z, E) + Q^+(z, E) - L(E)\Phi^+(z, E) \quad (1)$$

$$\frac{d\Phi^-(z, E)}{dz} = \sigma_2(z, E)\Phi^-(z, E) - \sigma_1(z, E)\Phi^+(z, E) - Q^-(z, E) + L(E)\Phi^-(z, E) \quad (2)$$

Here $\sigma_2(z, E)$ is the cross section describing the loss of flux in the energy range E to $E + dE$. $\sigma_1(z, E)$ is the cross section describing the elastic back-scattering of electrons, $Q(z, E)$ is the electron production rate in the range E to $E + dE$ due to ionization processes and cascading of electrons down in energy from higher energy bins, and $L(E)$ describes the losses due to a finite spacecraft velocity. The cross sections take into account ionization of the atmospheric neutral species, back-scatter of electrons by neutral and charged particles, elastic and inelastic collisions, cascading of electrons down in energy etc. The coordinate system is chosen such that the z -axis is along the magnetic field with Φ^+ streaming in the positive direction. To account for pitch angle effects, an average pitch angle of 54.76° was used. The equations in their detailed form, excluding the term describing losses due to finite spacecraft velocities, are discussed in detail in *Banks et al.* [1974].

The altitude domain is divided into two regions: one is between the lower altitude boundary (70 km) and the spacecraft altitude, and the other is between the spacecraft altitude and the upper altitude boundary (900 km). First, the differential electron flux of a beam emitted from the spacecraft is assumed at the spacecraft altitude. The beam may be emitted either up or down, but let us assume in the following that the beam is emitted down. The fluxes are then determined in the region between the lower boundary and the spacecraft altitude in the same way as was done for the case of auroral electron fluxes. Next, the upward return flux found at the spacecraft altitude is emitted upwards, and the flux equations are solved in the region from the spacecraft altitude and to the upper boundary. The downward flux generated at the spacecraft altitude is added to the beam flux and the procedure is repeated until satisfactory convergence is reached.

The effect of a finite spacecraft velocity has been approximated by the inclusion of the loss term $L(E)$ in equations (1) and (2). The loss term can be determined from the following considerations: The beam is assumed to fill a volume with the dimension dx perpendicular to the magnetic field. The spacecraft velocity component perpendicular to the magnetic field, v_\perp , gives rise to a perpendicular flux Φ_\perp through the area element $dx dz$ as seen in the spacecraft reference system. This flux is lost to the beam flux-tube and the loss term can be expressed as

$$L(E) = \frac{v_\perp}{v_{\parallel}} dx \quad (3)$$

where v_{\parallel} is the particle velocity along the field.

The electron beam flux is modelled by a Gaussian distribution in energy centered around 1 keV and with an energy width of 10%. The beam is assumed to fill a flux-tube with a dimension perpendicular to the magnetic field of 10 m, which corresponds to 4 beam electron gyro-radii (for 90° pitch angle). This choice of beam column width is in accordance with observations obtained in the Spacelab-2 experiment flown on the space shuttle [Frank et al., 1989] and in the ECHO-7 sounding rocket experiment [Winkler et al., 1989]. The beam is emitted downwards for the range of spacecraft altitudes and corresponding perpendicular velocities obtained in the CHARGE-2 experiment and it is assumed that the Mother collects only a small fraction of the return fluxes. The MSIS/86 model [Hedin, 1987] is used for the neutral atmosphere (N_2 , O_2 and O) and the IRI model [Bilitza, 1986] is used for the ionosphere. The models are those corresponding to the local time, season, geographic location etc. of the launch. The IRI model of electron densities compares well with the electron densities observed during the flight [Myers, 1989].

4. MODEL CALCULATIONS

An example of the differential energy flux spectrum obtained at the location of the Mother platform when it is at an altitude of 260 km is shown in Figure 3. The two components of the fluxes shown are the flux streaming in the direction of the beam (down) and the flux streaming counter to the beam (up). The downward flux consists of two contributions, the primary electron beam which is seen with a peak at the beam energy, and the flux incident from above the spacecraft, seen at lower energies.

The fluxes as a function of altitude and for fixed energies are shown in Figure 4a for the 1-keV electron beam energy and in Figure 4b for 10-eV electrons. The spacecraft altitude is again 260 km as indicated on the figures and the beam is emitted downwards. The downward flux shown in Figure 4a is discontinuous at the spacecraft altitude. This fact simply reflects the location of the beam source at this altitude. If aimed downwards, a spectrometer mounted on the spacecraft will observe a value of the back-scattered flux corresponding to Φ_{up} at the spacecraft altitude. If the spectrometer is aimed upwards and in the opposite direction to the beam it will observe a flux corresponding to the value of the upper branch of Φ_{down} at the spacecraft altitude. The downward flux shown in Figure 4b is continuous because no beam electrons are emitted at 10 eV.

As can be seen from Figures 4a and 4b, energetic electron fluxes are generated along the magnetic field out to considerable distances from the spacecraft. At low altitudes the electron fluxes approach zero and become omni-directional because of scattering in the dense atmosphere. The upward flux decreases relatively slowly with altitude. This effect is caused by a decrease in the ambient neutral density or an increase in the mean free path which allow the electrons to escape almost freely. Similarly, the downward electron flux increases from essentially zero at high altitudes to large values at lower altitudes. The creation of electron fluxes extending along the direction of the magnetic field both above and below the payload to distances far beyond the payload potential sheath region is in qualitative agreement with optical observations made during the Excede 2 [O'Neil *et al.*, 1978] and the Echo 7 [Winckler *et al.*, 1989] sounding rocket experiments.

The current densities, $J^{BAI}(z_0)$, at the spacecraft location, z_0 , can be found by integrating the return fluxes over energy. Since the fluxes and thereby the BAI return currents are proportional to the emitted beam current it is convenient to define the parameter Λ as the sum of the current densities from both directions normalized to the emitted beam current density.

$$\Lambda(z_0) = \frac{J_{down}^{BAI}(z_0) + J_{up}^{BAI}(z_0)}{J_{beam}} \quad (4)$$

As can be seen from (4), Λ represents a gain factor. In Figure 5 is shown the variation of Λ during the CHARGE-2 flight. The different values of Λ during the upleg and the downleg are caused by changes in v_{\perp} . During the upleg v_{\perp} was larger than during the downleg.

The values shown in Figures 3-5 have been calculated assuming that only a small fraction of the flux is collected by the spacecraft. As shown in Neubert *et al.* [1990] the sheath area of the Mother, A , is about 12.8 m^2 when charged to 400 V. With the assumption that the flux-tube cross-sectional area is 100 m^2 , the payload actually collects about 13% of the electrons in the flux-tube and thus the values shown in Figures 3-5 are slightly overestimated.

The return current to the Mother given by the NASCAP/LEO estimates (the passive current) is shown in Figure 6a as a function of the observed return current. For most of the values the model current is lower than the observed current. Extreme differences can be seen, especially for the data point marked with an asterisk. This observation was performed at a low altitude during the downleg. Here the model current is less than 1 mA while the observed return current was 36 mA.

Figure 6b shows an estimate of the return current when the BAI current is added to the passive current. The BAI current has been found from the relation

$$I_{BAI} = I_{beam} \cdot \Lambda \cdot \frac{A}{d^2} \quad (5)$$

As can be seen from Figure 6b, the agreement between this new model estimate of the return current and the observed return current is much better. The data point marked with an asterisk is now lifted to a value slightly larger than the observed value.

5. SUMMARY

Under the simple assumption that the beam flux-tube has a cross-sectional area of 100 m^2 , the total return current to the Mother payload is found to be in reasonable agreement with the observed return current. We also find that the predictions from the model of electron fluxes extending to large distances in the direction of the emitted beam as well as in the opposite direction is in qualitative agreement with optical observations performed in past experiments [O'Neil *et al.*, 1978; Winckler *et al.*, 1989]. Similarly, the prediction of electron fluxes incident on the spacecraft from both hemispheres is in qualitative agreement with observations [Winckler *et al.*, 1975]. A quantitative investigation of the BAI currents generated during electron beam emissions in experiments other than the CHARGE-2 experiment will be reported in a separate publication.

One of the main shortcomings of the model is the uncertainty of the cross-sectional area of the beam flux-tube and the variation of the electron fluxes across this area. A more rigorous treatment of the problem would involve Monte Carlo techniques to determine the dimension and the distribution of electrons across the flux-tube.

We have shown that a hot electron distribution will be generated by the BAI. The observations of a hot component is then not an immediate evidence for BPI. In fact, the hot component generated through BAI may dominate the cold ambient plasma component and therefore be important for a realistic model of BPI. To illustrate this, we show in Figure 7 the beam current, I_{limit} , defined as the beam current for which $I_{BAI} = I_{thermal}$, as a function of altitude. The arrows indicate the upleg and downleg portions of the curve. In the region of high beam current, to the right of the curve, the BAI current is larger than the thermal current. This implies that in this region the plasma in the flux-tube around the beam and the payload is dominated by a hot component. This will be the case in particular for the forth-coming Charge-2B rocket experiment scheduled for 1991. Here, it will be attempted to emit beams with energies of 3 keV and currents of 3 A, with neutral gas releases and thruster emissions as means of enhancing the return current collection to the spacecraft.

ACKNOWLEDGEMENTS

We are grateful for the support of Prof. Andrew Nagy and Dr. Janet Kozyra who made the original photo electron and auroral electron code available to us and helped us with many questions that came up during our effort to modify the code for artificial electron beams. The experimental work was sponsored by NASA and the Air Force Geophysical Laboratory under NASA grant NAGW-1566, by NASA under contracts NAS8-35350 and NAG5-607, and by RADC under contract F19628-89-K-0040.

REFERENCES

- Banks, P. M., C. R. Chappell, and A. F. Nagy, A new model for the interaction of auroral electron beams with the atmosphere: spectral degradation, backscatter, optical emission, and ionization, *J. Geophys. Res.*, **79**, 1459, 1974.
- Beard, D. B., and F. S. Johnson, Ionospheric limitations on attainable satellite potential, *J. Geophys. Res.*, **66**, 4113, 1961.
- Bilitza, D., International reference ionosphere: Recent developments, *Radio Sci.*, **21**, 343, 1986.
- Frank, L. A., W. R. Paterson, M. Ashour-Abdalla, D. Schreiver, W. S. Kurth, D. A. Gurnett, N. Omid, P. M. Banks, R. I. Bush, and W. J. Raitt, Electron velocity distributions and plasma waves associated with the injection of an electron beam into the ionosphere, *J. Geophys. Res.*, **94**, 6995, 1989.
- Gilchrist, B. E., P. M. Banks, T. Neubert, P. R. Williamson, N. B. Myers, W. J. Raitt, and S. Sasaki, Electron collection enhancement arising from neutral gas jets on a charged vehicle in the ionosphere, *J. Geophys. Res.*, **95**, 2469, 1990.
- Hedin, A. E., MSIS-86 thermospheric model, *J. Geophys. Res.*, **92**, 4649, 1987.
- Langmuir, I., and K. B. Blodgett, Current limited by space charge flow between concentric spheres, *Phys. Rev.*, **24**, 49-59, 1924.
- Linson, L. M., Charge neutralization as studied experimentally and theoretically, in *Artificial Particle Beams in Space Plasma Studies*, edited by B. Grandal, p. 573, Plenum Press, New York, 1982.
- Mandell, M. J., J. R. Lilley, Jr., I. Katz, T. Neubert, and N. B. Myers, Computer modelling of current collection by the CHARGE-2 mother payload, *Geophys. Res. Lett.*, **17**, 135, 1990.
- Myers, N. B., W. J. Raitt, B. E. Gilchrist, P. M. Banks, T. Neubert, P. R. Williamson, and S. Sasaki, A comparison of current - voltage relationships of collectors in the ionosphere with and without electron beam emission, *Geophys. Res. Lett.*, **16**, 365-368, 1989.
- Myers, N. B., Studies of the system-environment interaction by electron beam emission from a sounding rocket payload in the ionosphere, *Ph. D. Dissertation*, Utah State University, Center for Atmospheric and Space Sciences, Logan, Utah, 1989.
- Neubert, T., P. M. Banks, B. E. Gilchrist, A. C. Fraser-Smith, P. R. Williamson, W. J. Raitt, N. B. Myers, and S. Sasaki, The interaction of an artificial electron beam with the earth's upper atmosphere: Effects on spacecraft charging and the near-plasma environment, *J. Geophys. Res.*, *in press*, 1990.
- O'Neil, R.R., O. Shepherd, W. P. Reidy, J. W. Carpenter, T. N. Davis, D. Newell, J. C. Ulwick, and A. T. Stair, Jr., Excede 2 test, an artificial auroral experiment: Ground-based optical measurements, *J. Geophys. Res.*, **83**, 3281, 1978.
- Parker, L. W., and B. L. Murphy, Potential buildup on an electron-emitting satellite in the ionosphere, *J. Geophys. Res.*, **74**, 1631-1636, 1967.
- Sasaki, S., K. I. Oyama, N. Kawashima, T. Obayashi, K. Hirao, W. J. Raitt, N. B. Myers, P. R. Williamson, P. M. Banks, and W. F. Sharp, Tethered rocket experiment (Charge 2) - Initial results on electrodynamics, *Radio Sci.*, **23**, 975-988, 1988.
- Waterman, J., K. Wilhelm, K. M. Torkar, and W. Riedler, Space shuttle charging or beam-plasma discharge - what can electron spectrometer observations contribute to solving the question?, *J. Geophys. Res.*, **93**.

4134, 1988.

Winckler, J. R., R. L. Arnoldy, and R. A. Hendrickson, Echo 2: A study of electron beams injected into the high-latitude ionosphere from a large sounding rocket, *J. Geophys. Res.*, *80*, 2083, 1975.

Winckler, J. R., P. R. Malcolm, R. L. Arnoldy, W. J. Burke, K. N. Erickson, J. Ernstmeier, R. C. Franz, T. J. Hallinan, P. J. Kellogg, S. J. Monson, K. A. Lynch, G. Murphy, and R. J. Nemzek, ECHO 7 An electron beam experiment in the Magnetosphere, *EOS*, *70*, 657, 1989.

FIGURE CAPTIONS

Figure 1. Configuration of the CHARGE-2 payload and the electron current system around the payload during electron beam emissions. I_{beam} is the emitted beam electron current, I_{tether} is the electron current in the tether, I_M is the return current to the Mother, and I_D is the return current to the Daughter.

Figure 2. Tether to beam current ratio, I_{tether}/I_{beam} , as a function of altitude. SQ2 through SQ6 marks in time-sequential order the experimental sequences performed during the flight. Also indicated is the ratio of the Daughter collecting area to the total collecting area of Mother and Daughter, A_D/A_{total} .

Figure 3. The upward and the downward differential electron flux as a function of energy at the spacecraft altitude (260 km). The beam is emitted downward with an energy of 1 keV and a current of 100 mA (the fluxes scale linearly with the beam current). The primary beam is seen as the peak at 1 keV in the downward flux.

Figure 4. The differential electron fluxes as function of altitude for the same parameters used in Figure 3. (a) 1-keV electrons and (b) 10-eV electrons.

Figure 5. Λ as a function of altitude.

Figure 6. Model estimates of the return current to the Mother vs. observed return current. a) The model assumes passive current collection only (NASCAP/LEO estimates). b) The model includes passive and BAI return currents.

Figure 7. The beam current for which the thermal current to the Mother equals the BAI current as a function of altitude. The arrows indicate the upleg and downleg portions of the flight.

CHARGE - 2

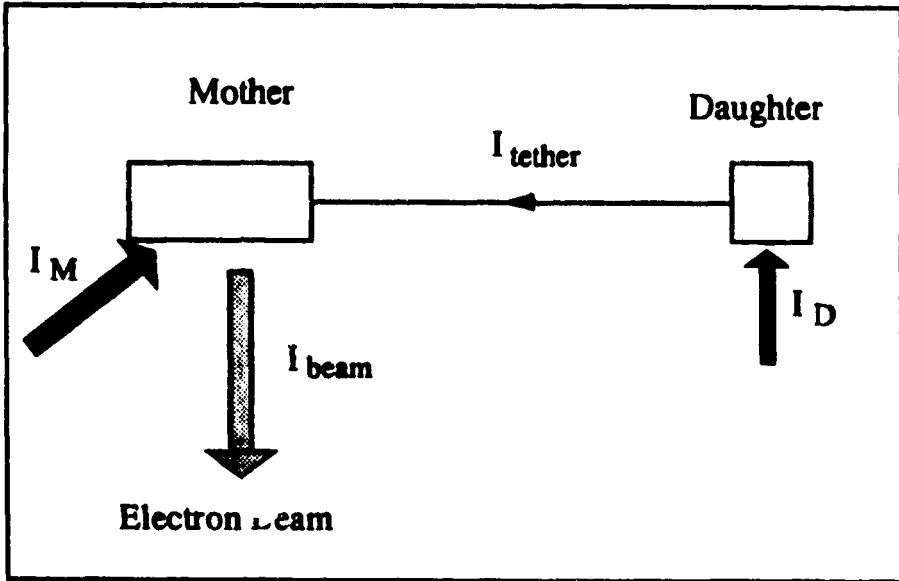


Figure 1

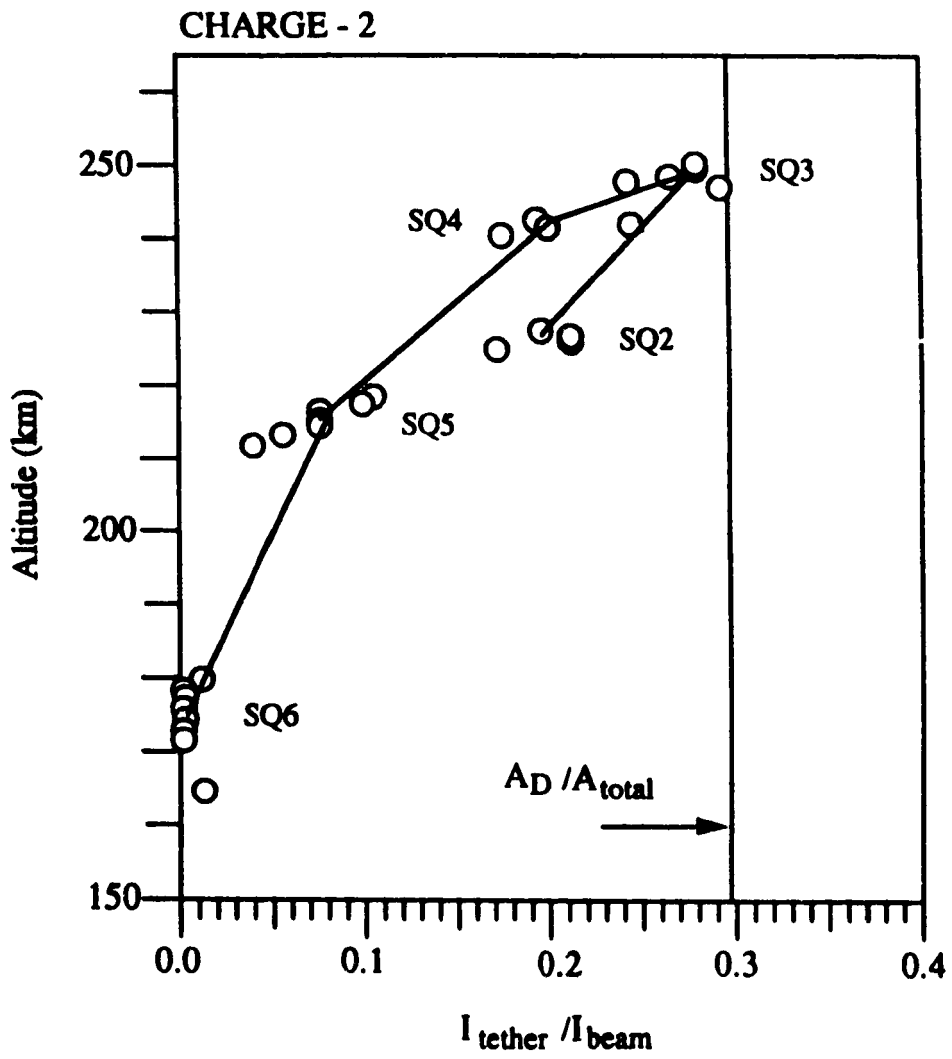


Figure 2

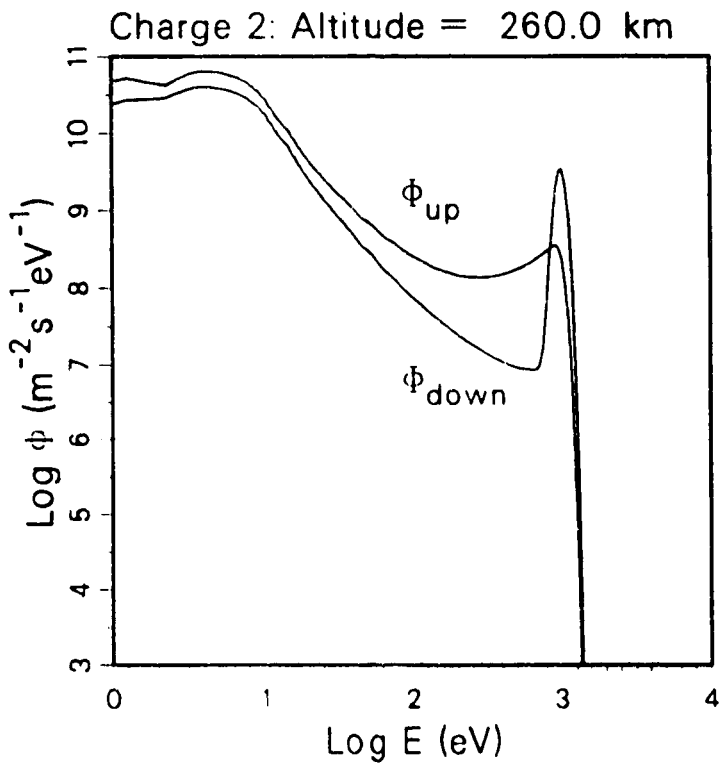


Figure 3

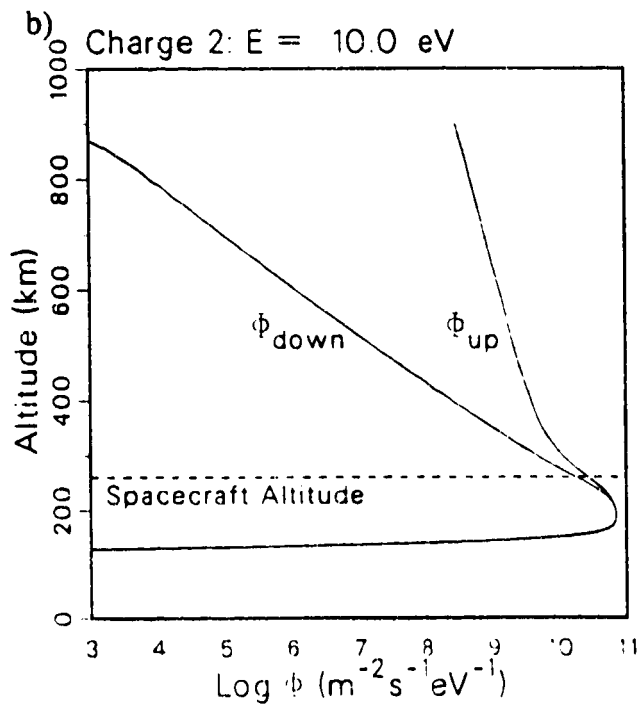
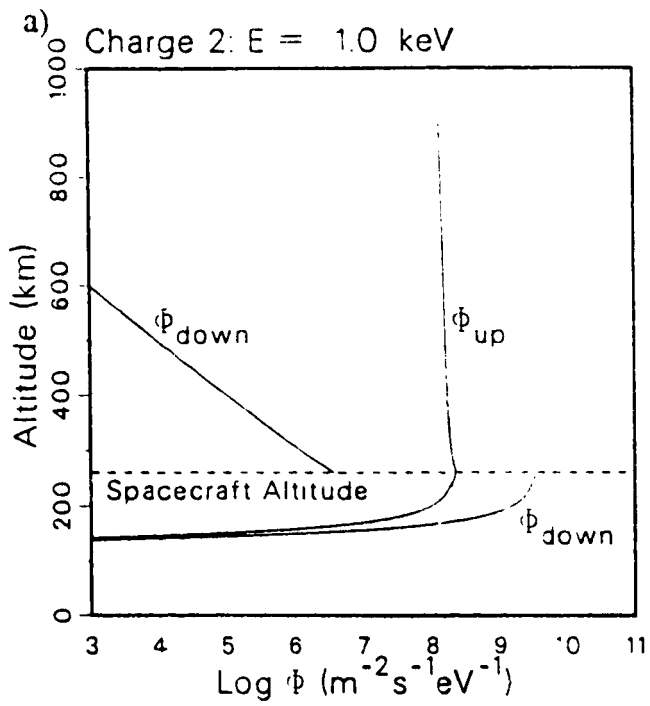


Figure 4

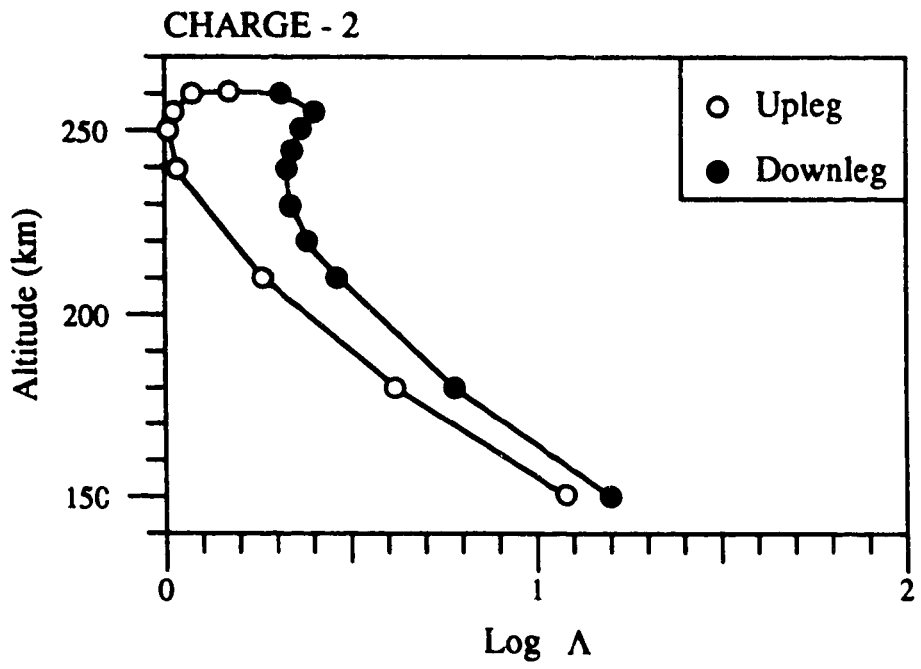


Figure 5

Figure 6a

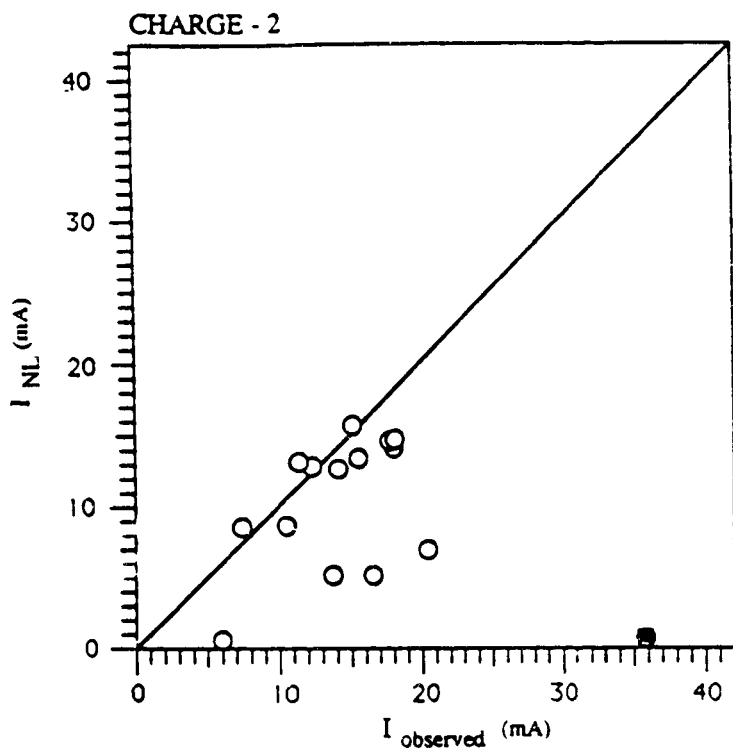
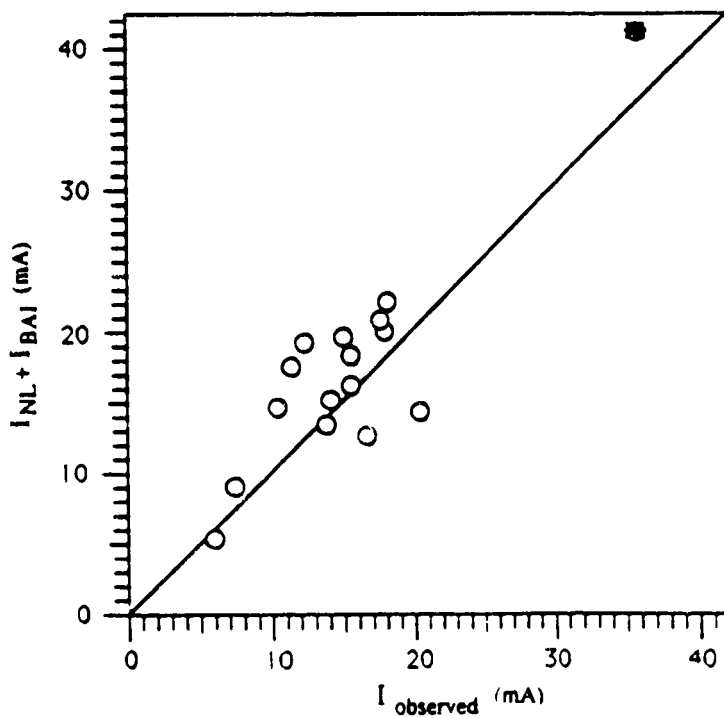


Figure 6b



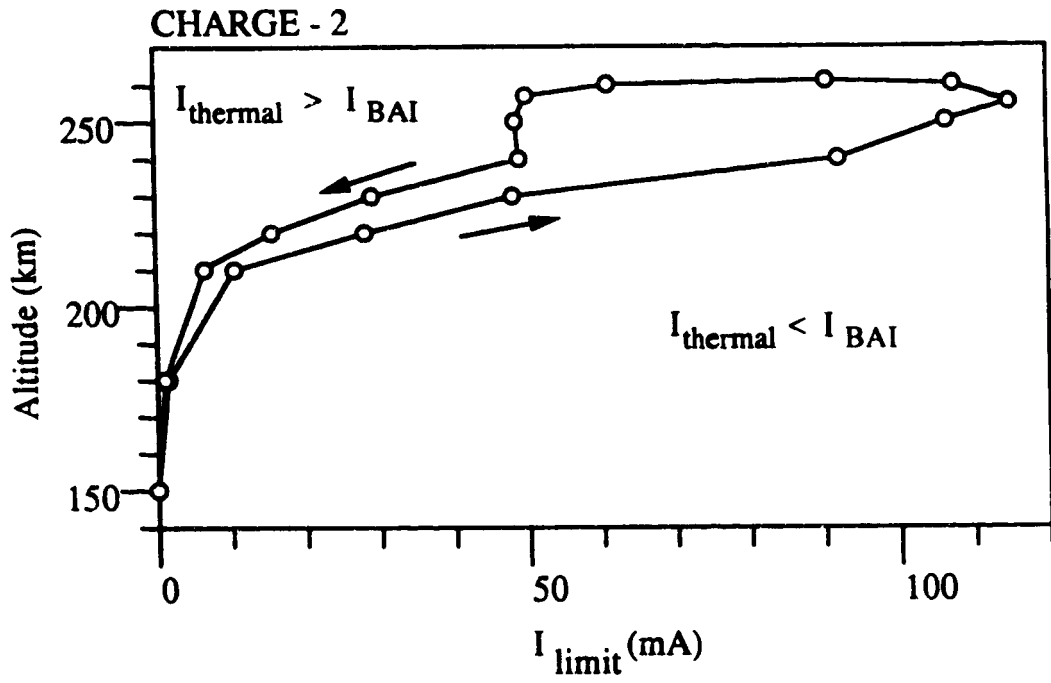


Figure 7